Quaternary Research 86 (2016) 348–358

Contents lists available at ScienceDirect

Quaternary Research

journal homepage: http://www.journals.elsevier.com/quaternary-research

New aspects of the interpretation of the loess magnetic fabric, Cérna Valley succession, Hungary

Balázs Bradák-Hayashi [a, b, *], Tamás Biró [c], Erzsébet Horváth [c], Tamás Végh [c], Gábor Csillag [d]

[a] Department of Planetology, Kobe University, 1-1, Rokkodai-cho, Nada-ku, Kobe, Hyogo, 657-8501, Japan
[b] Geographical Institute, Research Centre for Astronomy and Earth Sciences (HAS), 45 Budaörsi St., H-1112, Budapest, Hungary
[c] Department of Physical Geography, Eötvös Loránd University, 1/C Pázmány P. St, H-1117, Budapest, Hungary
[d] Geological and Geophysical Institute of Hungary, 14 Stefánia St., H-1143, Budapest, Hungary

ARTICLE INFO

Article history:
Received 9 November 2015
Available online 18 September 2016

Keywords:
Microfabric
Directional fabric
Photostatistics
Image analysis
Visible grain fabric
Micromorphology
Magnetic fabric

ABSTRACT

Anisotropy of magnetic susceptibility (AMS) is a frequently applied method in sedimentology, especially in the determination of the orientation of transport processes. We present an analysis of magnetic fabric (MF) studies on loess. New aspects of fabric development reveal: i) The deposition of the aeolian sediments was controlled by gravity, low-energy transport and local geomorphology, hence no clarified wind direction can be defined. ii) The influence of phyllosilicates is also significant among the magnetic components. iii) While the primary MF is relatively well-defined, the secondary MF is influenced by several processes. The analysis of stereoplots combined with the q–β diagram and photostatistics showed encouraging results during the characterization of various secondary MF such as redeposited MF and pedogenic fabric. iv) Changes in processes from aeolian to water-lain deposition and the increasing transportation energy were reflected by the connection between AMS and observed micro-scale sedimentary features. v) A relationship was obvious between the degree of pedogenesis and the transformation of sedimentary MF into a vertical MF typical for paleosols. vi) The significant role of very fine grained magnetite on the formation of inverse MF could not be excluded.

Introduction

There are two different main points of view on defining the primary (wind-blown, aeolian) magnetic fabrics (MF) of loess. Derbyshire et al. (1988) suggested that the fabric of aeolian loess is isotropic, and every anisotropy detected in the fabric is related to secondary processes. Hus (2003) and Wang and Løvlie (2010) pointed out that the gravitational force and compaction play the main role in developing the primary MF of loess.

In contrast to this theory, many studies have altered this perspective: the MF of 'wind-blown' loess is supposed to be anisotropic and the orientation of κ_{max} (maximum magnetic susceptibility) is fingerprinted by syn-depositional paleowind direction (e.g., Begét et al., 1990; Thistlewood and Sun, 1991; Sun et al., 1995; Wu et al., 1998; Lagroix and Banerjee, 2002, 2004; Zhu et al., 2004; Bradák, 2009; Zhang et al., 2010; Liu and Sun, 2012).

Deviation of the inclination of κ_{min} (minimum magnetic susceptibility) from vertical has been used to separate the fabrics of undisturbed (where wind-blown, the inclination of κ_{min} is less than 20°) from redeposited/reworked loess (e.g., Zhu et al., 2004). However, the pronounced deviation of κ_{min} from vertical is not necessarily the result of redeposition. If the sedimentation occurred on a slope, the dip direction of the paleosurface could be identified by the alignment of the principal susceptibilities: by the tilt of the κ_{min} directions from the vertical and by the inclination of the plane defined by the intermixed κ_{max} and κ_{int} (intermediate magnetic susceptibility) axes from the horizontal plane (e.g., Rees, 1966, 1971; Bradák et al., 2011; Bradák and Kovács, 2014; Ge et al., 2014).

A similar tilting of the foliation plane might also be the result of imbrication in the mass-flow just prior to the emplacement. In this case, the alignment of the principal susceptibilities show an a-axis type imbrication (elongated grains tend to align parallel with the transport direction and showing an upflow tilting).

* Corresponding author. Department of Planetology, Kobe University, 1-1, Rokkodai-cho, Nada-ku, Kobe, Hyogo, 657-8501, Japan.
E-mail address: bradak.b@people.kobe-u.ac.jp (B. Bradák-Hayashi).

http://dx.doi.org/10.1016/j.yqres.2016.07.007
0033-5894/

Thus, this fabric is similar to the former case (tilted fabric via deposition on a paleoslope), but it is the result of an opposite direction of transportation (e.g., Thistlewood and Sun, 1991; Nawrocki et al., 2006).

AB-plane imbrication, or 'pencil-fabric,' was found by Zeeden et al. (2015) in (typical?) loess MF. In 'AB-plane imbricated fabric', the a-axes of the clasts are aligned perpendicular to the flow direction and the intermediate axes are aligned in the direction of the flow. In the stereoplots of AB-plane imbricated fabric, the κ_{min} and κ_{max} directions are well clustered and intermixed on a plane with an inclination close to 90°. AB-plane imbricated magnetic fabrics were described in the studies of Tarling and Hrouda (1993) and Tauxe (1998), and their development is believed to indicate high-energy transport.

AB-plane imbrication was also observed in the MF of redeposited loess samples (Bradák et al., 2011). Based on the study of Zeeden et al. (2015), 'strong wind' could be responsible for the development of AB-plane imbrication. However, the rolling transportation (tracting) of the 'dust grain size' material and AB plane imbrication during aerial transport is questionable.

Post-sedimentary processes are also detectable by the analysis of the magnetic fabric. Deviations of κ_{min} from vertical were interpreted as a cryptic post-depositional deformation by permafrost processes (Lagroix and Banerjee, 2004; Taylor and Lagroix, 2015). Disturbed isotropic magnetic fabrics were observed in various paleosols (Matasova et al., 2001; Hus, 2003). Inverse magnetic fabric was also observed in paleosols (Matasova and Kazansky, 2004; Bradák et al., 2011). The term 'inverse fabric' has been used in the sedimentary fabric studies since the investigation of Rochette (1988). In this case, the direction of κ_{max} is perpendicular to the almost horizontal bedding plane (κ_{max} inclination ~ 90°). A serious problem could arise, however: the 'inverse fabric' can indicate both the vertical alignment of minerals and the crystallographic anisotropy of minerals such as fine-grained magnetite or siderite (Hrouda, 1982; Rochette, 1988; Márton et al., 2010).

The goal of this study was: i) Elaborate a micromorphological investigation and photostatistical analysis to revise and clarify the results of the AMS measurements of Cérna Valley samples; ii) reveal the relationship between some components of the paleoenvironment (e.g., mode of transportation, pedogenesis) and the MF; and iii) infer to the processes played major roles in the development of the magnetic fabrics in Cérna Valley sections.

Site and sampling

The Cérna Valley (Cérnavölgy) profile (47.3642730° N, 18.6025329° E) is located near the village of Vértesacsa in the eastern foreland of the Vértes Hills, Hungary (Fig. 1). The Plio-Pleistocene history of the studied area and a detailed description of the section and its surroundings are summarized by Budai et al. (2008) and Bradák et al. (2011). Based on lithostratigraphical and paleopedological correlations and the published chronometric data from the surrounding area (Thamó-Bozsó et al., 2010), the profile may be dated to the middle/late Pleistocene transition period and to the late Pleistocene.

The aim of the previous study of the Cérna Valley section was to reconstruct the paleoenvironment using environmental magnetic methods. Besides heavy-mineral, sedimentological, and paleomagnetic studies (Bradák et al., 2011), a systematic sampling was carried out for micromorphological analyses.

The micromorphological sampling followed the recent S exposure of the studied outcrop (W–E horizontal orientation of the samples). The W–E horizontal orientation of the samples coincided with the visible inclination of the layers as well (Bradák et al., 2011). The strike of the layers and the orientation of the possible transport processes could not be clearly determined in the field. The azimuth of the micromorphological samples could affect the results of the photostatistical analysis: weaker 'virtual' imbrication of the grains could be identified and compared to the 'real' imbrication.

Methods

New parameters for describing the distribution of principal susceptibilities

Two new parameters were applied for the revision of previous AMS results from Cérna Valley samples. The parameter 'q' ('shape factor') was introduced by Granar (1958). 'q' compares the intensity of magnetic lineation in the magnetic foliation plane with the intensity of the foliation (Taira, 1989):

$$q = L/F$$

where L is the magnetic lineation, defined by the formula of Balsley and Buddington (1960) and F is the magnetic foliation calculated by the formula of Stacey et al. (1960).

The 'β' (imbrication angle) was defined by:

$$\beta = 90 - \kappa_{min}\text{incl.}$$

where $90-\kappa_{min}$ incl. is the inclination of the minimum principal susceptibility. In this case, the angle of imbrication was defined by the tilt of the short axis (Taira, 1989).

The q–β diagram was applied by Taira (1989) to reveal the relationship between the angle of imbrication and the shape factor. The q and β values are known to be related to the gravitational and tangential stress forces in the production of the fabric (Taira, 1989). Various areas were separated on the diagram based on the specific β and q values related to different materials and transportation by aeolian or water-lain processes, thus various ratio of gravitational and tangential stress during transport (Fig. 2a), and deposition in various environments was characterized by various sedimentary structures (e.g., horizontal lamination, tabular and trough cross-bedding) (Fig. 2b). The range of q for different sediments, collected by von Rad (1970), is also depicted on the diagram (Fig. 2c).

Photostatistical analysis of thin sections

Image analysis of 15 microphotographs (with 1200 × 1600 pixel resolution) of oriented thin sections was performed to obtain information on visible clast fabric defined by the azimuths of the longest axes (a-axes) of grains. The digitalisation of individual grains was performed using Adobe Photoshop CS5.1. To obtain measurable polygons from the grains, ENVI EX 4.6 software was used. The azimuths of the a-axes and elongation (a-axis/b-axis) values were determined using ArcMap 10.0 software. To evaluate the fabrics, circular frequency diagrams (rose diagrams) of the azimuths were produced with GEOrient 9.5 software.

In all samples, some grains with a perfectly square shape were identified, characterized by an azimuth of either 0.0 or 90.0°. To eliminate the contribution and biasing effect of such grains, circular frequencies excluding these values were also compiled. Among the 'normal' distributions, circular frequencies weighted by the elongation values (Davis, 1986), and rose diagrams of grains with elongation values higher than 2.0 were also created to obtain more reliable information on possible shearing directions. More elongated grains are better indicators of the principal direction of shearing, because they tend to spend more time in the position of lowest angular velocity (flow- or shear-parallel, e.g., Bhattacharyya,

https://doi.org/10.1016/j.yqres.2016.07.007 Published online by Cambridge University Press

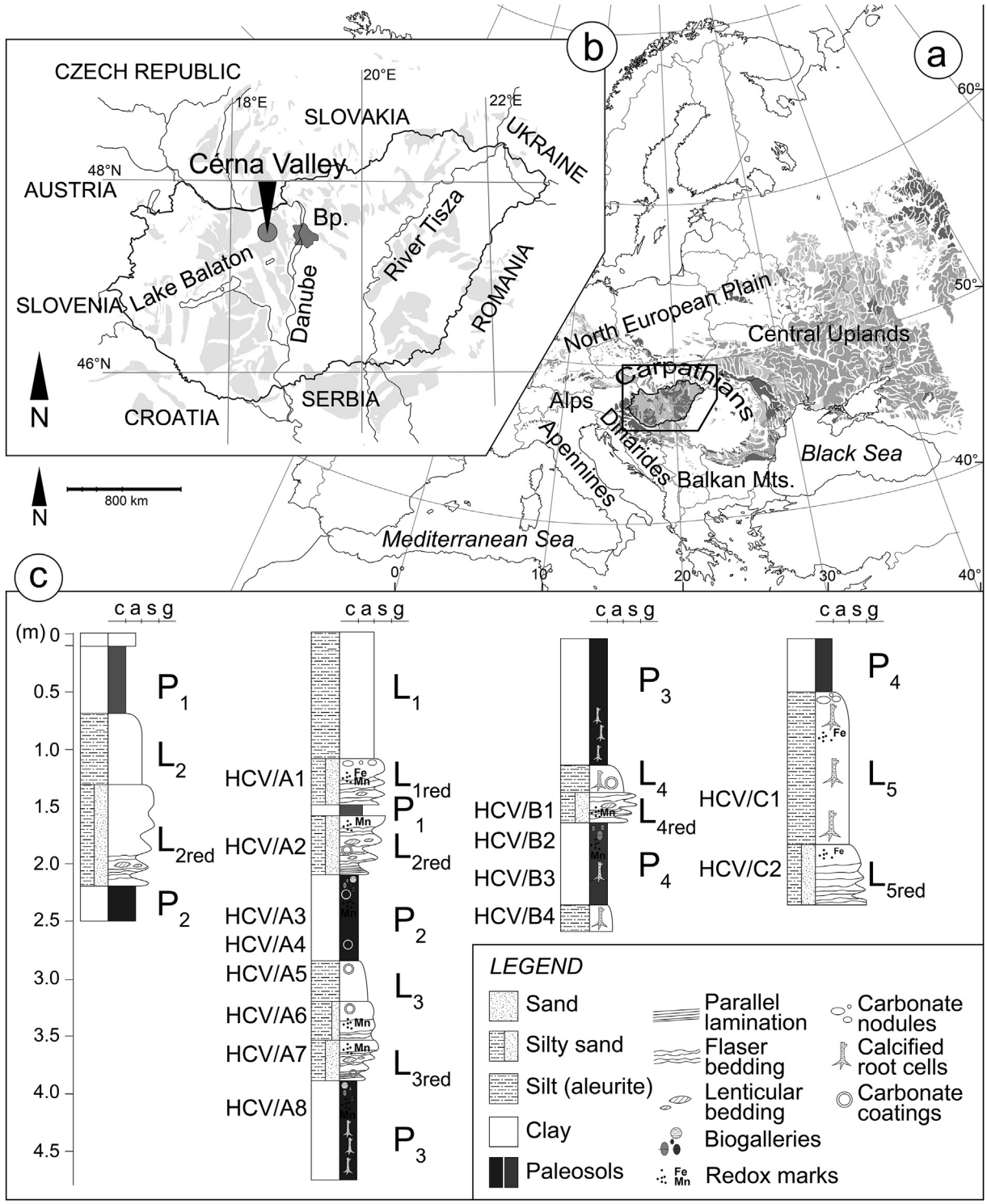

Figure 1. The locality of Cérna Valley section in European Loess Belt (a) and in Hungary (b), and the graphic plot of the investigated profile with the sampling points (c). The map of European Loess Belt based on the map published in Haase et al. (2007). The gray-colored polygons show the loess areas.

1965; Rees, 1968, 1979). The number of such grains analysed in the investigated populations ranges from 8 to 10,933.

In samples where ped or soil fragments were present, the fabric of matrix grains and grains from peds was determined separately. In addition, bulk fabrics containing all grains from both the matrix and ped fragments were interpreted.

The spatial pattern of the grain a-axis directions was studied by a 'grain vector map,' which is constructed from the micromorphological thin sections. The following steps were carried out in order to calculate and then visualize the a-axis directions of the analysed grains in ArcMap 10.0 software:

i) 'Zonal Geometry' from 'Table Tool' in ArcMap 10.0 was used to calculate the orientation of the a-axes of grains from a vertical base direction in a counter-clockwise (CCW) direction.

https://doi.org/10.1016/j.yqres.2016.07.007 Published online by Cambridge University Press

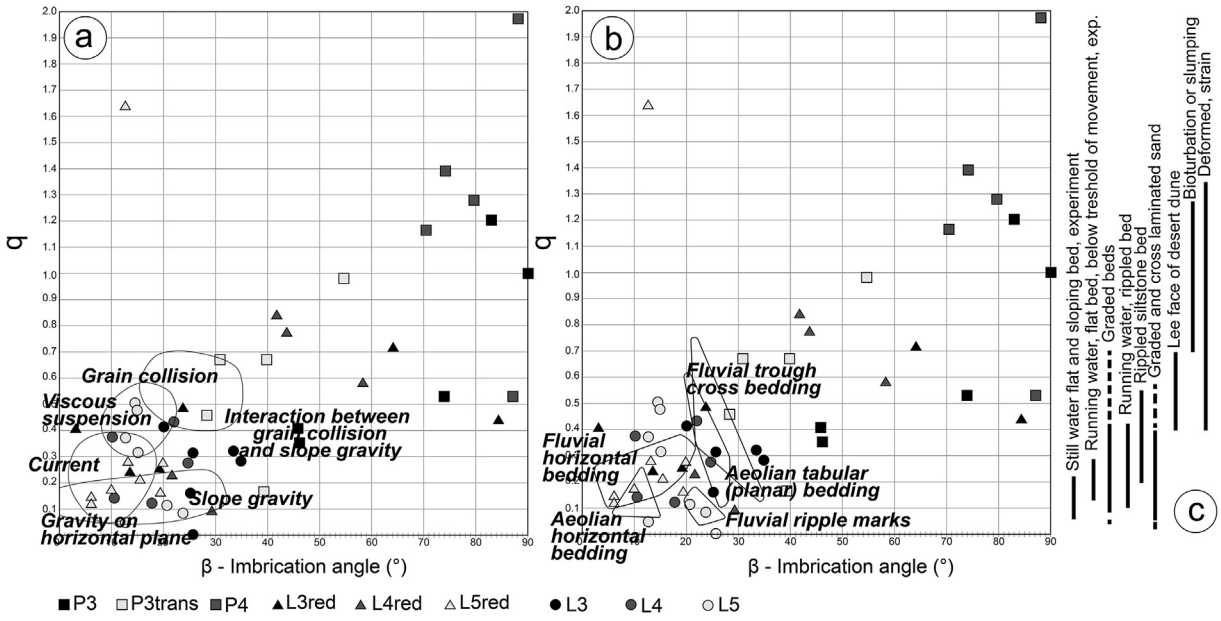

Figure 2. The β vs. q (Taira) diagram.

ii) The end-points of individual grains' long axes were calculated.
iii) A vector between the centroid and the endpoints for each grain by using the 'XY to line' tool was generated.

The result of this process was an 'a-axis vector map', where each vector corresponds to the a-axes of a grain.

The goal of the performed photostatistical analyses was to reveal the visible two-dimensional grain fabric in order to obtain a dataset quasi-suitable for comparison with the three dimensional magnetic fabric. Please note that the following factors can theoretically bias the visible fabric:

- Due to the differences between the orientation (strike) and the dimensions of the micromorphological (W/E and 2D) and magnetic fabric samples (NE/SW and 3D; Bradák et al., 2011), the comparison of the results has some limitations and possibly contains some errors. However, large grain populations decrease the effect of such errors.
- The shape, and thus the orientation, of the smaller grains can be distorted and simplified by the various software processing steps (e.g., raster-vector conversion). Each microphotograph was recorded using the same magnification and resolution. Thus, the relative resolution (with respect to the average grain size) allows more precise grain boundary detection in samples with coarser grains. In the case of smaller average grain sizes, the circular frequencies and the preferred directions are supposed to be more uncertain. This 'random' orientation of the small grains could result in a nearly isotropic background which tends to 'dilute' the actual preferred iso-orientation of the larger grains (for more information see Supplementary material 1). In conclusion, we believe that the circular frequencies that contain only the most elongated grains ($e > 2.0$) are the most accurate indicator of the directional fabric.

Micromorphology

One of the most commonly used methods in paleoenvironmental reconstruction from loess and paleosol series is micromorphological study (e.g., Tsatskin et al., 1998; Kemp, 1999; Terhorst et al., 2014, 2015). 'Brick-like', vertically originated samples were taken from some sediments and paleosols for meso- and micromorphological examination (Fig. 1). In the course of the mesomorphological examination, the samples were analyzed using an Olympus B061 binocular microscope. Oriented 6 × 9 cm 'mammoth' thin sections were prepared from samples for micromorphological description.

The analysis of the micromorphological thin sections was based on the studies of Bullock et al. (1985), Kemp (1999), Kemp et al. (2006), Tsatskin et al. (1998) and Stoops et al. (2010). During the systematic analysis of the thin sections, the nomenclature of Bullock et al. (1985) was used (Supplementary material 1 and 2). Based on the results of the analysis, the micromorphological soil development index (MISODI) was determined to quantify the intensity of the post-sedimentary alteration and the degree of pedogenesis (Magaldi and Tallini, 2000).

The detailed description of the micromorphological character of the studied layers is presented in Supplementary material 1–4. The significant micromorphological features from a 'fabric development' point of view, were emphasized and are summarized in the Discussion chapter.

Results

The q–β (Taira) diagram

The Cérna Valley samples shows the following β and q parameters, which could be transferred to possible depositional environments, processes and energies on the basis of von Rad (1970) and Taira (1989):

- The 'wind-blown' loess samples were characterized by relatively low imbrication angle (~10–25°) and foliated magnetic fabric ($q < 0.5$). That the redeposited loess samples showed more significant scattering and similar or higher absolute β (~5–85°) and q (0.1–0.5 and 1.7 in one sample) values than in aeolian loess is evident. The paleosols were characterized by the highest β (30–90°) and q (0.15–1.4 and 2.0 in one sample) values and fabrics, with the dominance of lineation compared to foliation.

https://doi.org/10.1016/j.yqres.2016.07.007 Published online by Cambridge University Press

- No distinct boundary between the area of loess variations and paleosol fabrics could be defined.
- Based on the magnetic fabrics related to specific sedimentary structures (Fig. 2a), the scattered values of homogeneous loess (L3, L4, L5) fell into several categories: 'aeolian horizontal and tabular (planar) bedding', 'fluvial horizontal bedding' and 'fluvial ripple marks'. The laminated loess samples (L3red, L4red, L5red) mainly plotted in the 'fluvial horizontal bedding' category.
- On the basis of magnetic fabrics, which are typical for specific sedimentary processes, environments and transportation energies, the samples fell into different categories (Fig. 2b). According to the diagram, the magnetic fabric of 'wind-blown' loess developed under the influence of gravity (on horizontal plane or slope) and deposited from an environment whose physical properties resemble a 'viscous suspension'. The 'interaction between grain collision and slope gravity' could have also had some influence on the alignment of the magnetic grains. On the contrary, the redeposited loess samples mainly fell into the category of the materials deposited by 'currents'.
- Some redeposited loess samples and the paleosols could not be classified based on the categories of Taira (1989) ('uncategorized' on Fig. 2a and b).
- Due to the overlap of q values, the q of homogeneous and laminated loess samples is similar to various sediments (e.g., flat and sloping bed, ripple bed, graded bed sediments) published by von Rad (1970) (Fig. 2). The higher q values of paleosols are possibly related to the effect of bioturbation based on the comparison of the data from Cérna Valley and von Rad (1970).

Results of the photostatistical analysis

Considering the fabric directions indicated by different circular frequency diagrams (bulk, filtered, elongation-weighted, e > 2.0) (Fig. 3), nearly all samples are characterized by a good agreement

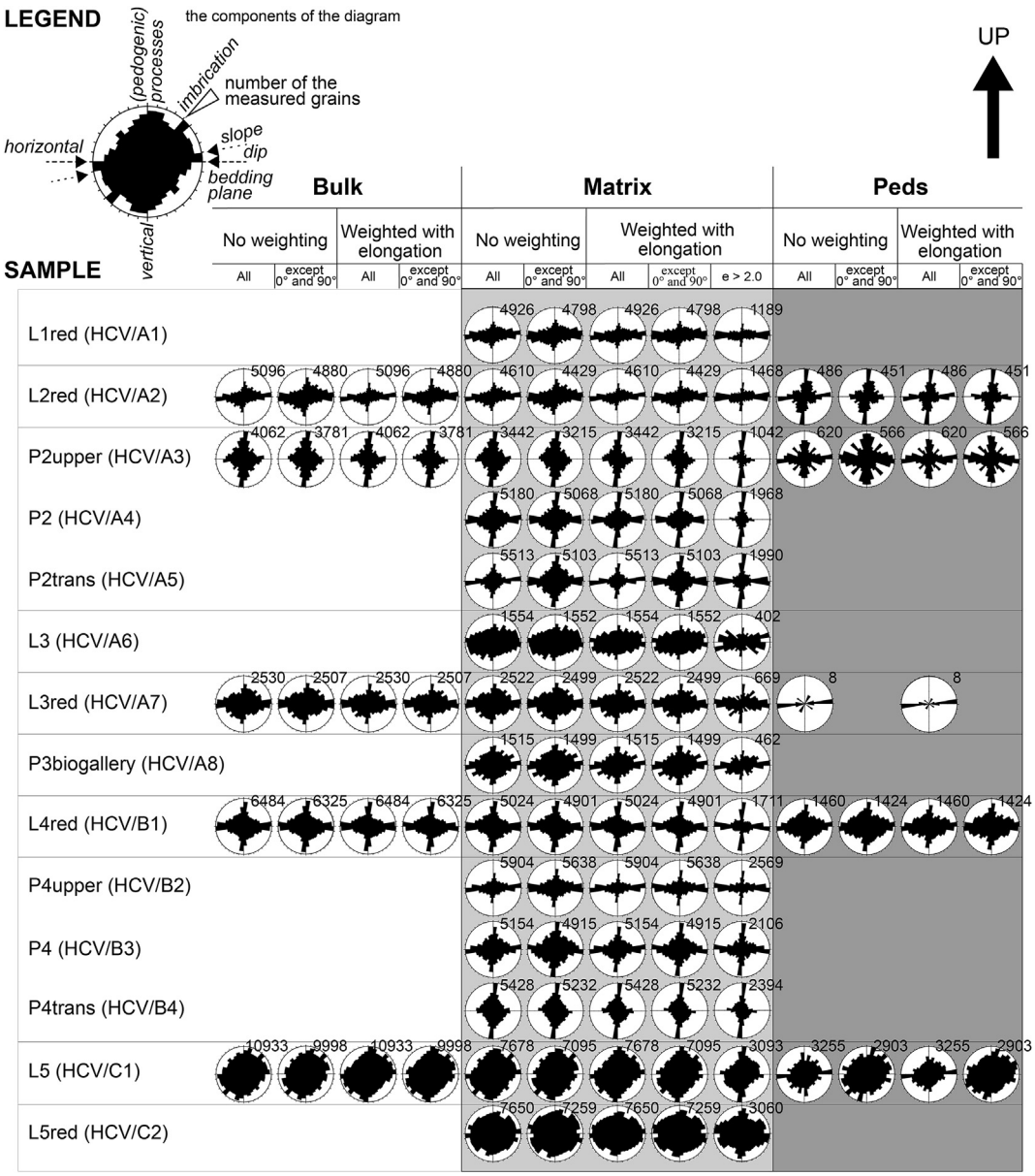

Figure 3. Results of photostatistical analysis plotted on circular frequency diagrams. In each cases data for the grains of the loess were separated from the grains in the ped fragments. See the text for further explanation on the methodology.

https://doi.org/10.1016/j.yqres.2016.07.007 Published online by Cambridge University Press

within samples. The only exception is the P2 (HCV/A4) sample, where the 'matrix, non-weighted' and 'matrix, elongation-weighted' distributions show a 0–180° and 90–270° bidirectional fabric (Fig. 3). On the contrary, the e > 2.0 distribution is characterized by a clear 0–180° unimodal fabric direction.

In all cases, the e > 2.0 populations show the strongest isoorientation in the sense of clustering around a preferred direction. The basic fabric properties (fabric strength, type of anisotropy, direction of preferred orientation) are interpreted on the basis of the circular frequencies of grains with e > 2.0 (Table 1). Regarding the fabric's strength, the distributions could be classified into strongly, moderately, and weakly anisotropic and isotropic clusters. Most of the distributions show unimodal anisotropy, where one preferred fabric direction is evident, but in some cases bimodal anisotropies define vertical and horizontal preferred directions are also present.

The orientation of grains from ped fragments shows isotropic distribution except in two samples. In the case of L2 (HCV/A2), a weakly anisotropic distribution with vertical and horizontal preferred directions is evident. The L3red (HCV/A7) sample is characterized by a very good horizontal anisotropy; however, only 8 ped fragments were included in the evaluation, thus this distribution cannot be regarded as representative.

The analysis of the 'grain vector maps' of micromorphological thin sections showed complex distribution patterns of a-axis directions for various layers (for the 'a-axis vector maps' see the Supplementary material 4 and Fig. 4). The circular frequency diagram and the a-axis vector map of the macroscopically homogeneous samples also show a weak orientation and somewhat weak a-axis imbrication (e.g., Figs. 3 and 4a, L3 sample). The mutual representation of vertical and horizontal subfabric on the a-axis vector map of the paleosol samples (Fig. 4b) is well reflected by the bimodal character of the circular frequency diagram (Fig. 4, P2, P4 samples). On the a-axis vector map of the transition layers (e.g., P2trans, P4upper and P4transpaleosol horizons), the representation of the nearly orthogonal subfabrics mentioned above also appeared on various scales (Figs. 3 and 4b). The grain vector map of the redeposited materials (e.g., L2red, L3red and L5red) is also characterized by a complex fabric in the case of the grains: the redeposited samples have (strongly) imbricated and/or laminated microfabrics (Figs. 3 and 4c). Besides the grain orientation due to sedimentary processes, the a-axis vector map of the sample, which consisted of ped fragments, could also be characterized by chaotic, isotropic vector orientation.

Discussion

Three components that are contributing to the magnetic susceptibility signal of the samples were identified by Bradák et al. (2011): two of these are the multidomain ferromagnetic (magnetite or maghemite) component identified by IRM studies and the superparamagnetic component identified by frequency dependence of magnetic susceptibility (κFD%) as well as 'fading of intensity' after magnetization. In addition to the dominant magnetite, the presence of haematite is also indicated by the high HIRM% in the fabric of homogeneous loess. The paleosol layers are characterized by the highest magnetic susceptibility, due to the higher concentration of multidomain ferromagnetic grains and the superparamagnetic components (Bradák et al., 2011).

Pearson's correlation method and correlation matrix (Supplementary material 5 and 6, Fig. 5) was applied to reveal the relationship between various sedimentary and post-sedimentary processes and the magnetic fabric properties, and synthesize the results of the complex, AMS, micromorphology and visible grain fabric investigation. The following datasets were used during the analysis: the AMS parameters (F, L, P, q, β), MISODI and the phyllosilicate ratio from micromorphological investigation, the photostatistical grain-size and elongation parameters calculated from the polygons of a-axis vector map, and the grain-size distribution,

Table 1
Basic fabric properties of the investigated distributions of grain orientations.

Sample	Fabric strength	Type of anisotropy	Direction of preferred orientation, and the indicated process
L1red (HCV/A1) L2red (HCV/A2)	Strong Strong	Unimodal Unimodal[a]	Gently dip angle, deposition on slope and/or marks of imbrication-like orientation of grains due to the gravity derived grain realignment after deposition
P2upper (HCV/A3)	Strong	Unimodal	Horizontal, the horizontally oriented sedimentary fabric was overwritten by the vertical oriented grains (pedogenic processes)
P2 (HCV/A4) P2trans (HCV/A5)	Strong Strong	Bimodal Bimodal	Horizontal and vertical; the parallel appearance of the primary sedimentary (horizontal) and the secondary, pedogenic orientation (vertical). In the lowest pedogenic horizon (P2trans) the influence of the pedogenic processes was decreasing, the amount of horizontal and vertical oriented grains were equal.
L3 (HCV/A6)	Moderate	Unimodal	Horizontal, foliated grain orientation with the possible appearance of A-axis imbrication
L3red (HCV/A7)	Weak	Unimodal	Weak horizontal grain orientation with the increasing amount of imbricated and some nearly vertical grains
P3biogallery (HCV/A8)	Moderate	Unimodal	Horizontal grain orientation but stronger imbrication and vertical (pedogenic?) component
L4red (HCV/B1)	Strong	Bimodal	Vertical and horizontal; mixed fabric of the accumulated horizon with vertical oriented biogalleries and the overlaying sediment with nearly horizontal grains
P4upper (HCV/B2) P4vertical (HCV/B3) P4trans (HCV/B4)	Strong Moderate Strong	Unimodal Bimodal Unimodal	The change of the fabric of a paleosol from the upper pedogenic horizon with the horizontal grain of the overlaying materials, through the middle pedogenic horizon with the change of the fabric due to the vertical pedogenic processes, to the lower horizon with the dominance of the
L5 (HCV/C1)	Very weak (isotropic)	–	The appearance of A-axis imbrication (scattered 0–30° dip of grains), none the less the well oriented magnetic fabric, very weak fabric by photostatistical analysis
L5red (HCV/C2)	Very weak (isotropic)	–	–

[a] A weaker vertical preferred direction is also remarkable.

https://doi.org/10.1016/j.yqres.2016.07.007 Published online by Cambridge University Press

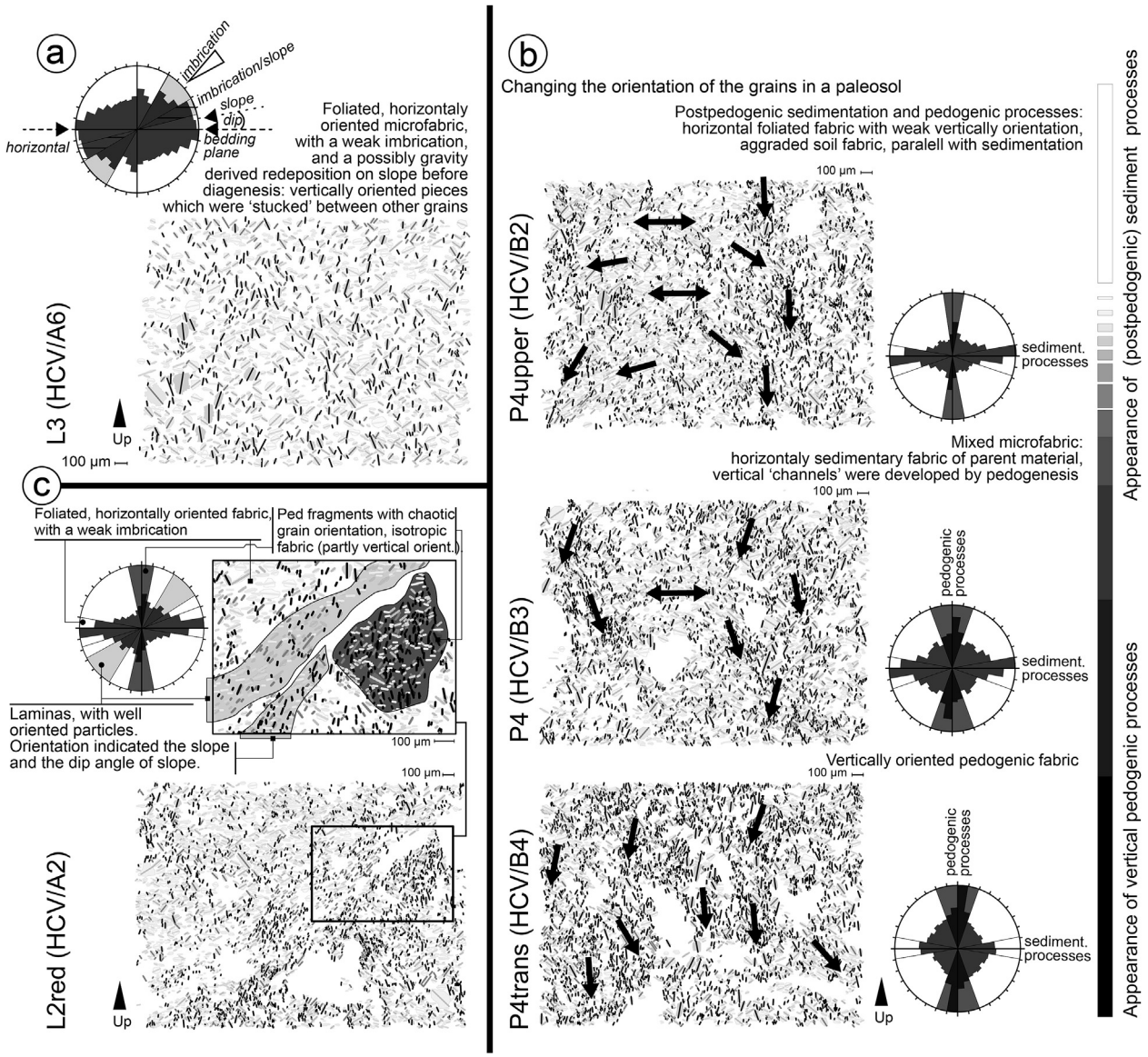

Figure 4. A-axes vector map of loess (a), paleosol (b) and redeposited loess (c) samples. Legend: 0.0–15.0° and 165.0001–180.0°–lightest gray color; 15.0001–30.0 and 150.0001–165.0° –light gray color; 30.0001–45.0° and 135.0001–150.0° – middle gray color; 45.0001–60.0° and 120.0001–135.0° –darker gray color; 60.0001–75.0° and 105.0001–120.0° – darkest gray color; 75.0001–105.0° – black color.

mineral composition and κFD% from Bradák et al. (2011) (Table 1, Supplementary material 1–6, Figs. 5 and 6):

- The change of the F and the P showed strong relationship ($r = 0.77$ and 0.75 respectively) with the amount of the (coarse) silt fraction (Bradák et al., 2011) (Fig. 5a). In addition, a negative relationship was revealed between the ratio of clay fraction and the F ($r = -0.73$) and the P ($r = -0.72$) values. The correlation between the grain-size distribution revealed by photostatistics (Supplementary materials 5) and the AMS parameters also indicated a relationship. There is a significant connection between the amount of (coarser) silt size components (~24.2–37.1 μm) and F ($r \sim 0.5$–0.75) (Fig. 5b).
- The various parameters indicated quasi-horizontally deposited (aeolian, wind-blown loess) imbricated materials or slope deposition (Figs. 3 and 6) (aeolian- and redeposited, water-lain loess also). The weak magnetic fabric orientation (scattered κ_{max} on stereoplots) (Fig. 6), the strong foliation of the fabric, the homogeneous 'microsedimentary' structure (Supplementary material 4, e.g., L3, L5), the circular frequency diagrams (Fig. 3) and the q–β diagram (Fig. 2) all together indicated a calm, mainly gravity-dominated depositional environment during the deposition of the aeolian loess.
- The predominantly silt-sized grains were compacted after the accumulation, which resulted in the well-foliated magnetic fabric a preferred horizontal a-axis direction on the vector maps and rose diagrams (Supplementary material 4, Fig. 6).
- The accumulation of the sediment on the slope was detected by the inclination of κ_{min} from the vertical (Fig. 6; L3, L5). In the case of the Cérna Valley section, the supposed regional prevailing wind direction was NW to SE during the Pleistocene (Sebe et al., 2011). In contrast to the prevailing wind direction, the accumulation of the dust was possibly dominantly affected by local palaeogeomorphology: the material is supposed to have been accumulated on SW-facing paleoslopes of NW-oriented ridges according to the orientation of κ_{min} inclination from vertical.

https://doi.org/10.1016/j.yqres.2016.07.007 Published online by Cambridge University Press

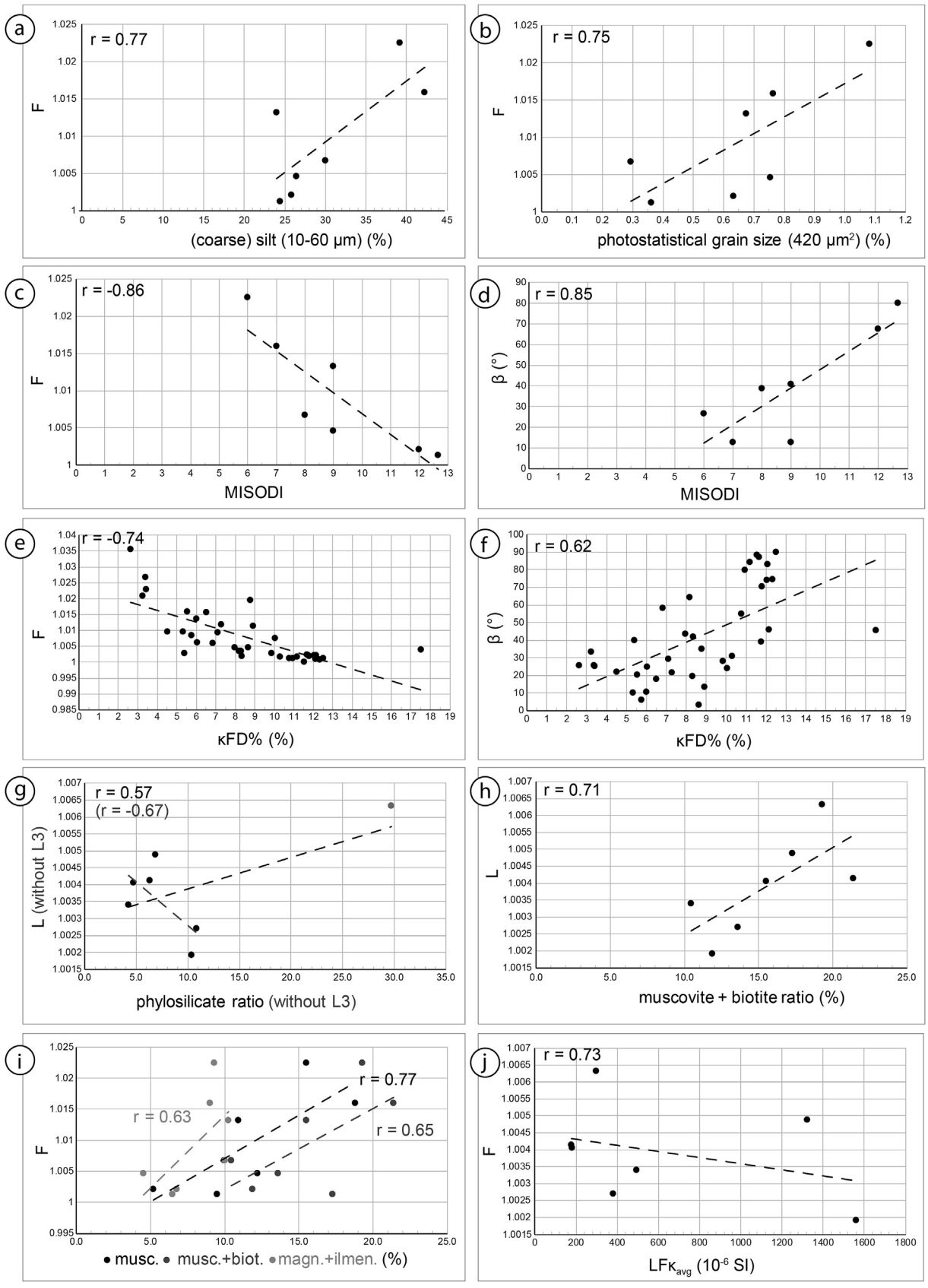

Figure 5. The results of Pearson's correlation: a, (coarse) silt vs. F (based on the grain-size data of Bradák et al. (2011)); b, photostatistical coarse silt vs. F; c, MISODI vs. F; d, MISODI vs. imbrication angle (β); e, frequency dependence of magnetic susceptibility (κFD%) vs. F (Bradák et al., 2011); f, frequency dependence of magnetic susceptibility (κFD%) vs. β; g, phyllosilicate ratio (based on micromorphological thin section) vs. L; h, muscovite + biotite ratio (Bradák et al., 2011) vs. L; i, mineral ratios (Bradák et al., 2011) vs. F; j, average low field magnetic susceptibility ($LF\kappa_{avg}$) vs. F.

https://doi.org/10.1016/j.yqres.2016.07.007 Published online by Cambridge University Press

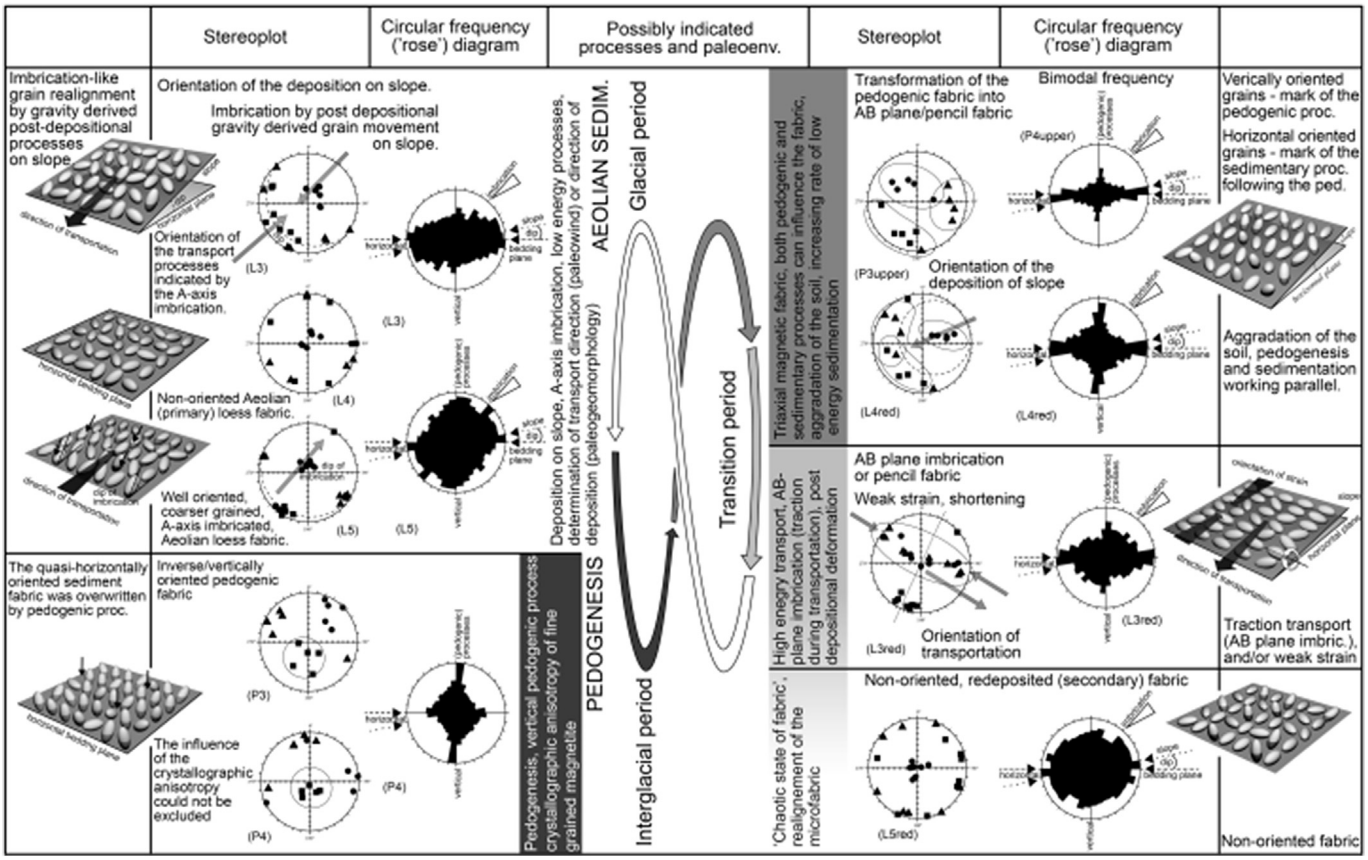

Figure 6. The synthesis of the results of the magnetic fabric studies and the micromorphological/photostatistical analysis. The direction of principal susceptibilities is plotted on lower hemisphere stereographical projection, geographical coordinate system. ■ −maximum susceptibility, ▲ −intermediate susceptibility, ● −minimum susceptibility.

- Complex development of the MF during redeposition was revealed by the analysis in L3red and L4red redeposited loess samples (Fig. 6). Poorly sorted, poorly compacted, complex mixed type bedding (well-laminated fabric with the subordinate appearance of flaser-, and lenticular bedding) was observed in the L3red samples (Supplementary material 1–4). The lineated AB-plane imbricated magnetic fabric of L3red (Figs. 2 and 6) was developed via higher energy (water-lain) processes (e.g., Tarling and Hrouda, 1993; Tauxe, 1998).

The imbrication of the grains is evident on the circular frequency diagrams (Fig. 3, e.g., L1red, L2red and L3red samples; Fig. 4). The higher impact of surface processes was coupled with decreasing biogenic component in the fabric-forming forces (e.g., decreasing amount of carbonated root cells) as well (Supplementary material 1, 2 and 4). The magnetic fabric of L4red was characterized by weak lineation and moderate clustering of the principal susceptibilities (Fig. 6).

The common appearance of the pedal structures and the indicators of sedimentation processes (Fig. 3) suggest i) continuous pedogenesis during the transition phase between the interglacial and the glacial period or ii) the influence of the paleocurrents and water-lain sedimentation (q−β diagram; Fig. 2).

- The non-oriented, horizontally foliated fabric of L5red was moderately sorted, fine grained (micro)laminated and moderately compacted. The grains were partly cemented by secondary carbonate impregnations (Supplementary material 1–4). No clear direction of deposition could be identified via the distribution of principal susceptibilities on stereoplots. The redeposited magnetic fabric is characterized by a significant anisotropy in the sense of κ_{min} clustering (Fig. 6). Contrastingly, the photostatistical analysis showed an almost isotropic microfabric (Figs. 3 and 6) and similarly chaotic grain fabrics within the moderately sorted ped fragments.

During the transition phase between the pedogenic (interglacial, interstadial) and aeolian sedimentation (glacial, stadial) period, the alignment of the magnetic minerals can become chaotic or triaxial by the change of environment (e.g., rising transport energy). From this chaotic state, the minerals can be rearranged by new processes, such as compaction, redeposition or pedogenic processes.

- A strong negative relationship was observed between the MISODI and the F and P ($r = -0.86$ and $r = -0.84$, respectively) (Fig. 5c). The influence of the pedogenesis was also indicated by the strong relationship between the MISODI and q ($r = 0.84$), and the β ($r = 0.85$) as well (Fig. 5d). During the development of the paleosol, the quasi horizontally aligned grains of the MF were supposed to be mixed up and realigned by vertical pedogenic processes (e.g., mineral migration, vertical water infiltration and desiccation cracks by the change of the water content).

The vertical orientation (high β values) of the pedogenic fabrics and the character of the pedogenic processes were characterized

https://doi.org/10.1016/j.yqres.2016.07.007 Published online by Cambridge University Press

by: i) the significant lineation of the magnetic fabric, ii) greater variability in the degree of the spreading of κ_{max} on stereoplots compared to sedimentary fabrics, and iii) the inclination of the κ_{max} from horizontal (Fig. 5; P3upper, P3 and P4). iv) Vertical shearing (associated with pedogenic processes) generally fingerprinted the circular frequencies of a-axis orientations as well, which shows a significant vertical iso-orientation (Figs. 3 and 4). v) The impact of the pedogenesis and the dominance of the vertical transport processes (e.g., clay migration) is also indicated by the presence of pedogenesis-related micromorphological features (ped structures, vertical orientation of striated birefringence (b-) fabric; Supplementary material 1–4). The pedogenesis and the vertical orientation of the magnetic grains was also indicated by the $q - \beta$ diagram (Fig. 2). Based on the results of the correlation of the frequency dependence of magnetic susceptibility (κFD%; Bradák et al., 2011) and the AMS parameters, the influence of the inverse crystallographic anisotropy of very fine grained magnetite cannot be absolutely excluded. The increase of κFD% (very fine grained pedogenic magnetite) is clearly coupled with decreasing F ($r = -0.74$) (Fig. 5d) (transformation of sedimentary fabric) and increasing β ($r = 0.62$; Fig. 5) (Fig. 5e) (indicator of inverse fabric).

- The influence of the paramagnetic phyllosilicates in the MF cannot be excluded due to the high ratio of biotite and muscovite identified in micromorphological thin sections (Supplementary material 2, 3 and 4), and is also indicated by the strongly oblate fabric of aeolian loess (Jelinek diagram in Martín-Hernández and Hirt, 2003; Bradák et al., 2011). The phyllosilicate ratio possibly causes the increase/decrease of L and P (Supplementary material 6, Fig. 5) based on the Pearson's correlation ($r = 0.57/-0.67$) (Fig. 5g); however, confusing results were revealed due to the influence of the high phyllosilicate ratio identified in L3 (29.7%; Supplementary material 6; Fig. 5f). The correlation of various mineral fractions (Bradák et al., 2011) and the AMS parameters clarified the results of micromorphological data (Fig. 5h and i): the higher ratio of the phyllosilicates possibly causes increase of the F ($r_{mu} = 0.77$; $r_{mu+bi} = 0.65$) and also the L ($r_{mu+bi} = 0.71$) of the materials.

The influence of the paramagnetic components on the magnetic fabric of materials with low susceptibilities ($\kappa_{avg} < 5 \times 10^{-4}$) was observed by Rochette (1987) and Hrouda and Jelinek (1990). In the case of the Cérna Valley samples, a strong relationship was revealed between the κ_{avg} and F ($r = 0.71$; Fig. 5) (Fig. 5j) that could indicate the influence of the phyllosilicates on the loess fabric ($\kappa_{avg\ loess} = \sim 2-3 \times 10^{-4}$).

Conclusion

A combined magnetic fabric, visible grain fabric via photostatistical analysis, and micromorphological characterization of Hungarian loess variations from the Cérna Valley loess/paleosol section was performed. Some new aspects of the development of the magnetic fabric of loess were revealed by the synthesis of the AMS, micromorphological, and photostatistical results (Fig. 6).

The aeolian sediment was deposited in calm environment, and in the case of Cérna Valley loess, the development of the primary (aeolian origin) magnetic fabric was mainly dominated by gravitational processes (e.g., dustfall without strong orientation). The orientation of the primary magnetic fabric is possibly influenced by the high ratio of detrital paramagnetic phyllosilicates (biotite, muscovite), by strong compaction during (post)diagenesis and also by the local geomorphological features (i.e., deposited on a slope).

In comparison with the aeolian loess, the development of secondary loess fabric (redeposited or altered primary fabric) could be influenced by numerous processes, such as gravitational processes, redeposition by wind, or water-lain processes, and also by pedogenesis. Based on the Cérna Valley study, there is no clear way to separate the primary and secondary fabrics.

The analysis of the alignment of principal susceptibilities combined with the q–β diagram showed promising results in the separation of aeolian and water-lain processes. The MF analysis, completed by micromorphology and photostatistics, clearly showed the changing of transport processes as the increase of transport energy during the development of the fabric.

Two main possible components were identified in the secondary fabric of paleosols: i) vertically oriented coarser components, reoriented by pedogenic processes, and ii) *in situ*-formed, very fine grained pedogenic components with inverse crystallographic anisotropy.

The magnetic fabric parameters of paleosols, via the disturbance of the magnetic fabric and the vertical orientation, would be a good tool to estimate the degree of pedogenesis in future AMS studies. It is revealed by the recent study that the complex micromorphological and photostatistical analyses, combined with magnetic mineralogical studies, would be feasible for the accurate determination of the origin of vertically oriented fabric.

The measurement of the anisotropy of magnetic susceptibility is a useful method to obtain basic three-dimensional information about the fabric of the loess variations and paleosols. Unfortunately, as the recent study shows, the application of this method has some limitation in loess research and needs more critical analysis during the interpretation of the AMS data, especially during the determination of the paleowind direction.

The new observations and interpretation suggest that surface processes and/or the paleogeomorphology play a more pronounced role during the deposition of the dust and during the post-depositional period, such as pedogenesis during the interglacial periods and redeposition during the transition phase between glacials and interglacials, than previously believed (e.g., Bradák et al., 2011; Bradák and Kovács, 2014; Ge et al., 2014; Taylor and Lagroix, 2015).

Also, care must be taken during the determination of the transport directions from the primary aeolian fabric due to the possible influence of the paramagnetic phyllosilicates, revealed by the reinterpretation of the AMS data, completed by micromorphological and grain orientation results. However, more targeted investigations of the paramagnetic fabric are needed to clearly define the character of the phyllosilicate influence on the loess MF.

The recent study has shown that the comparison of AMS parameters and non-magnetic methods, such as micromorphology and photostatistical analysis, would be helpful for the future loess magnetic fabric studies.

Acknowledgment

We are thankful for the paleomagnetic measurements in the Paleomagnetic Laboratory of the Geological and Geophysical Institute of Hungary. We are also thankful to Derek Booth, Jaime Urrutia Fucugauchi and the anonymous reviewers for their helpful comments. Balázs Bradák-Hayashi is an International Research Fellow of the Japan Society for the Promotion of Science (JSPS), who's fellowship at Department of Planetology, Kobe University, Japan was supported by the Japan Society for the Promotion of Science (JSPS).

Appendix A. Supplementary material

Supplementary material related to this article can be found at http://dx.doi.org/10.1016/j.yqres.2016.07.007.

References

Balsley, J.R., Buddington, A.F., 1960. Magnetic susceptibility anisotropy and fabric of some adirondack granites and orthogneisses. American Journal of Science 258, 6–20.

Begét, J.E., Stone, B.D., Hawkins, B.D., 1990. Paleoclimatic forcing of magnetic susceptibility variations in Alaskan loess during the late Quaternary. Geology 18, 40–43.

Bhattacharyya, D.S., 1965. Orientation of mineral lineation along the flow direction in rocks. Tectonophysics 3, 29–33.

Bradák, B., 2009. Application of anisotropy of magnetic susceptibility (AMS) for the determination of paleo-wind directions during the accumulation period of Bag Tephra, Hungary. Quaternary International 198, 77–84.

Bradák, B., Kovács, J., 2014. Quaternary surface processes indicated by the magnetic fabric of undisturbed, reworked and fine-layered loess in Hungary. Quaternary International 319, 76–87.

Bradák, B., Thamó-Bozsó, E., Kovács, J., Márton, E., Csillag, G., Horváth, E., 2011. Characteristics of Pleistocene climate cycles identified in Cérna Valley loess–paleosol section (Vértesacsa, Hungary). Quaternary International 234, 86–97.

Budai, T., Császár, G., Csillag, G., Fodor, L., Gál, N., Kercsmár, Zs., Kordos, L., Pálfalvi, S., Selmeczi, I., 2008. Geology of the Vértes Hills. Explanatory Book to the Geological Map of the Vértes Hills (1: 50 000), p. 368. Budapest.

Bullock, P., Fedoroff, N., Jongerius, A., Stoops, G., Tursina, T., 1985. Handbook for Soil Thin Section Description. Waine Research Publications, Wolderhampton, p. 152.

Davis, J.C., 1986. Statistics and Data Analysis in Geology, second ed. John Wiley & Sons, New York.

Derbyshire, E., Billard, A., Vliet-Lanoe, B.V., Lautridou, J.-P., Cremaschi, M., 1988. Loess and paleoenvironment some results of a European joint programme of research. Journal of Quaternary Science 3, 147–169.

Ge, J., Guo, Z., Zhao, D., Zhang, Y., Wang, T., Yi, L., Deng, C., 2014. Spatial variations in paleowind direction during the last glacial period in north China reconstructed from variations in the anisotropy of magnetic susceptibility of loess deposits. Tectonophysics 629, 353–361.

Granar, L., 1958. Magnetic measurements on Swedish varved sediments. Arkiv Geofysik 3, 1–40. In: Hrouda, F., (Ed.) 1982. Magnetic anisotropy of rock and its application in geology and geophysics. Geophysical Survey 5, 37–82.

Haase, D., Fink, J., Haase, G., Ruske, R., Pécsi, M., Richter, H., Altermann, M., Jäger, K.-D., 2007. Loess in Europe—its spatial distribution based on a European loess map, scale 1:2,500,000. Quaternary Science Reviews 26, 1301–1312.

Hrouda, F., 1982. Magnetic anisotropy of rock and its application in geology and geophysics. Geophysical Survey 5, 37–82.

Hrouda, F., Jelinek, V., 1990. Resolution of ferromagnetic and paramagnetic anisotropies in rock, using combined low-field and high-field measurements. Geophysical Journal International 103, 75–84.

Hus, J.J., 2003. The magnetic fabric of some loess/paleosol deposits. Physics and Chemistry of the Earth 28, 689–699.

Kemp, R.A., 1999. Micromorphology of loess-paleosol sequences: a record of paleoenvironmental change. Catena 35, 179–196.

Kemp, R.A., Zárate, M., Toms, P., King, M., Sanabria, J., Arguello, G., 2006. Late Quaternary paleosol, stratigraphy and landscape evolution in the Northern Pampa, Argentina. Quaternary Research 66, 119–132.

Lagroix, F., Banerjee, S.K., 2002. Paleowind direction from the magnetic fabric of loess profile in central Alaska. Earth and Planetary Science Letters 195, 99–102.

Lagroix, F., Banerjee, S.K., 2004. Cryptic post-depositional reworking in aeolian sediments revealed by the anisotropy of magnetic susceptibility. Earth and Planetary Science Letters 224, 453–459.

Liu, W., Sun, J., 2012. High-resolution anisotropy of magnetic susceptibility record in the central Chinese Loess Plateau and its paleoenvironment implications. Science China, Earth Sciences 55, 488–494.

Magaldi, D., Tallini, M., 2000. A micromorphological index of soil development for the Quaternary geology research. Catena 41, 261–276.

Martín-Hernández, F., Hirt, A.M., 2003. The anisotropy of magnetic susceptibility in biotite, muscovite and chlorite single crystals. Tectonophysics 367, 13–28.

Márton, E., Bradák, B., Rauch-Włodarska, M., Tokarski, A.K., 2010. Magnetic anisotropy of clayey and silty members of tertiary flysch from the Silesian and Skole Nappes (outher Carpathians). Studia Geophysica et Geodaetica 54, 121–134.

Matasova, G., Kazansky, A.Y., 2004. Magnetic Properties and Magnetic Fabrics of Pleistocene Loess/Palaeosol Deposits along West-Central Siberian Transect and Their Palaeoclimatic Implications, vol. 238. Geological Society, London, pp. 145–173. Special Publications 2004.

Matasova, G., Petrovský, E., Jordanova, N., Zykina, V., Kapička, A., 2001. Magnetic study of late Pleistocene loess/palaeosol sections from Siberia: palaeoenvironmental implications. Geophysical Journal International 147, 367–380.

Nawrocki, J., Polechońska, O., Boguckij, A., Łanczont, M., 2006. Palaeowind directions recorded in the youngest loess in Poland and western Ukraine as derived from anisotropy of magnetic susceptibility measurements. Boreas 35, 266–271.

Rees, A.I., 1966. The effect of depositional slopes on the anisotropy of magnetic susceptibility of laboratory deposited sands. Journal of Geology 74, 856–867.

Rees, A.I., 1968. The production of preferred orientation in a concentrated dispersion of elongated and flattened grains. Journal of Geology 76, 457–465.

Rees, A.I., 1971. The magnetic fabric of sedimentary rock deposited on slope. Journal of Sedimentary Petrology 41 (1), 307–309.

Rees, A.I., 1979. The orientation of grains in a sheared dispersion. Tectonophysics 55, 275–287.

Rochette, P., 1987. Magnetic susceptibility of the rock matrix related to the magnetic fabric studies. Journal of Structural Geology 9, 1015–1020.

Rochette, P., 1988. Inverse magnetic fabric in carbonate-bearing rocks. Earth and Planetary Science Letters 90, 229–237.

Sebe, K., Csillag, G., Ruszkiczay-Rüdiger, Zs., Fodor, L., Thamó-Bozsó, E., Müller, P., Braucher, R., 2011. Wind erosion under cold climate: a Pleistocene periglacial mega-yardang system in central Europe (western Pannonian basin, Hungary). Geomorphology 134, 470–482.

Stacey, F.D., Joplin, G., Lindsay, J., 1960. Magnetic anisotropy and fabric of some foliated rock from S.E. Australia. Geofisica Pura e Applicata 47, 30–40. In: Hrouda, F. (Ed.), 1982: Magnetic anisotropy of rock and its application in geology and geophysics. Geophysical Survey 5, 37-82.

Stoops, G., Marcelino, V., Mees, F., 2010. Interpretation of Micro-morphologicalFeaturesof Soils and Regoliths. Elsevier, p. 720.

Sun, J.M., Ding, Z.L., Liu, T.S., 1995. Primary application of magnetic fabric mensuration of loess and paleosols for reconstruction of winter monsoon direction. Chinese Science Bulletin 40 (21), 1976–1978 (in Chinese) in: Tang, Y., Jia, J., Xia, X. 2003. Record of properties in Quaternary loess and its paleoclimatic significance: a brief review. Quaternary International 108, 33–50.

Taira, A., 1989. Magnetic fabrics and depositional processes. In: Taira, A., Masuda, F. (Eds.), Sedimentary Facies in the Active Plate Margin. Terra Scientific Publishing Company, Tokyo, pp. 43–77.

Tarling, D.H., Hrouda, F., 1993. The Magnetic Anisotropy of Rock. Chapman – Hall, London, Glasgow, New York, Tokyo, Melbourne, Madras, p. 217.

Tauxe, L., 1998. Paleomagnetic Principles and Practice. Kluwer Academic Publishers, Dordrecht, Boston, London, p. 299.

Taylor, S.N., Lagroix, F., 2015. Magnetic anisotropy reveals the depositional and post-depositional history of a loess-paleosol sequence at Nussloch (Germany): AMS of Nussloch loess-paleosol sequence. Journal of Geophysical Research: Solid Earth 120. http://dx.doi.org/10.1002/.

Terhorst, B., Kühn, P., Dammc, B., Hambach, U., Meyer-Heintze, S., Sedov, S., 2014. Paleoenvironmental fluctuations as recorded in the loess-paleosol sequence of the Upper Paleolithic site Krems-Wachtberg. Quaternary International 351, 67–82.

Terhorst, B., Sedov, S., Sprafke, T., Peticzka, R., Meyer-Heintze, S., Kühn, P., Solleiro Rebolledo, E., 2015. Austrian MIS 3/2 loess–palaeosol records—key sites along a west–east transect. Palaeogeography, Palaeoclimatology, Palaeoecology 418, 43–56.

Thamó-Bozsó, E., Csillag, G., Fodor, L., Müller, P., Nagy, A., 2010. OSL-dating the Quaternary landscape evolution in the Vértes Hills forelands (Hungary). Quaternary Geochronology 5, 120–124.

Thistlewood, L., Sun, J.A., 1991. Paleomagnetic and mineral magnetic study of loess sequence at Liujiapo, Xi'an, China. Journal of Quaternary Science 6, 13–26.

Tsatskin, A., Heller, F., Hailwood, E.A., Gendler, T.S., Hus, J., Montgomery, P., Sartori, M., Virina, E.I., 1998. Pedosedimentary division, rock magnetism and chronology of the loess/palaeosol sequence at Roxolany (Ukraine). Palaeogeography, Palaeoclimatology, Palaeoecology 143, 111–133.

von Rad, U., 1970. Comparison between "magnetic" and sedimentary fabric in graded and cross-laminated sand layers, Southern California. Geologische Rundschau 60, 331–354.

Wang, R., Løvlie, R., 2010. Subaerial and subaqueous deposition of loess: experimental assessment of detrital remanent magnetization in Chinese loess. Earth and Planetary Science Letters 298, 394–404.

Wu, H.B., Chen, F.H., Wang, J.M., 1998. A study on the relationship between magnetic anisotropy of modern eolian sediments and wind direction. Chinese Journal of Geophysics (ACTA GeophysicaSinica) 41, 811–817 (in Chinese) in: Tang, Y., Jia, J., Xia, X., 2003. Record of properties in Quaternary loess and its paleoclimatic significance: a brief review. Quaternary International 108, 33–50.

Zeeden, C., Hambach, U., Händel, M., 2015. Loess magnetic fabric of the Krems-Wachtberg archaeological site. Quaternary International 372, 188–194.

Zhang, R., Kravchinsky, V.A., Zhu, R., Leping, Y., 2010. Paleomonsoon route reconstruction along a W-E transect in the Chinese Loess Plateau using the anisotropy of magnetic susceptibility: summer monsoon model. Earth and Planetary Science Letters 299, 436–446.

Zhu, R., Liu, Q., Jackson, M.J., 2004. Paleoenvironmental significance of the magnetic fabric of Chinese loess-paleosols since the last interglacial (<130 ka). Earth and Planetary Science Letters 221, 55–69.